2008

Integrated True-time Delay Unit for Broadband Inteference Nulling in Phased-array Antenna

Budi Juswardy
Edith Cowan University

Kamal Alameh
Edith Cowan University

10.1109/OECCACOFT.2008.4610466

Integrated True-time Delay Unit for Broadband Inteference Nulling in Phased-array Antenna

Budi Juswardy and Kamal Alameh
Centre of Excellence for Microphotonic Systems, Edith Cowan University, Joondalup WA 6027, Australia
Phone: +61863045146 Fax:+61863 045302 Email: bjusward@student.ecu.edu.au

Abstract - This paper discusses an integrated true-time delay generation unit based on microminiaturisation of photonic and electronic components. The design, simulation, and performance of important building blocks for implementing a true-time delay-based phased-array antenna are presented.

Introduction

The ability of an electronically programmable phased-array antenna to adaptively scan radiated beams in three-dimensional space without mechanically moving the antenna makes it suitable for attaining high signal-to-noise ratio, improved reliability and low transmission power. Most of the research on phased-array antenna has been focused on broadband beam steering and less attention has been given to null beamforming, which is the ability to place broadband nulls at chosen angular coordinates to minimise interference signals [1]. Broadband null steering requires a beamformer that can generate variable and frequency independent true time-delays. This requirement is difficult to achieve using conventional electronic phase-shifter circuits or Digital Signal Processors (DSP) [2].

Recent advances in microelectronics and fibre-optic telecommunications have enabled the fabrication of high-quality integrated circuits and photonic components, and opened up opportunities to merge electronics and optics for broadband signal processing [3]. A MicroPhotonic beamformer, which integrates microelectronics and photonics, has attractive features such as size miniaturisation, broadband frequency range, and multi-functional signal processing capability.

In this paper, we report on the design, development and characterization of the main components required for the implementation of an innovative MicroPhotonics-based wideband null-steering beamformer.

Proposed Adaptive Phased-array Null Beamformer

The architecture for the proposed MicroPhotonic adaptive phased-array antenna is illustrated in Fig. 1. Since the transmitter and receiver operations are conceptually similar, only receive-mode will be discussed. In receive-mode, antenna array elements receive the incoming signal, which is then split into K_N signal via the electronic splitter. Each of these K_N signals is modulated and converted to the optical domain via a Vertical Cavity Surface Emitting Laser (VCSEL) array and routed into a multi-cavity optical substrate, which generates a large number of different true time-delayed versions of modulated optical beams.

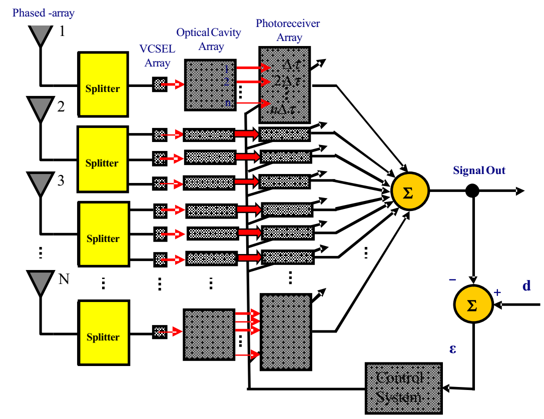

Fig. 1. MicroPhotonic adaptive phased-array null beamformer architecture.

Photoreceiver arrays convert these modulated light beams back into electronic signals and combine them to produce the signal output. The amplitude of the combined output signal depends on the direction of the received signal and the delay profile of the beamformer.

The Array Factor (directional response) of an N-element phased-array antenna is given by [2]:

$$AF_N(\theta) = \prod_{n=1}^{N-1}\left(x - x_n\right) = \sum_{m=0}^{N-1} W_m x^m \qquad (1)$$

where $x = \exp\left|-jkd\sin(\theta)\right|$, d is sensor element spacing, k = wave number = ω/c, and $x_n = x(\theta_n)$ = zero of AF_N corresponding to a null at angular coordinate θ_n. Note that a change of even one zero (or null direction) affects all the weights, W_m. Generally, for an N-element broadband phased-array antenna, the synthesis of $(N-1)$ zeros becomes feasible if the beamformer can adaptively generate and combine $(2^{N-1}-1)$ delayed versions of the incoming signals received by the antenna elements [1].

Figure 2 shows the interface between the VCSEL/photoreceiver chip and the optical substrate, and also illustrates the propagation of the optical beams inside the optical substrate. Each VCSEL element generates a laser beam that is modulated by the incoming RF signal associated to this VCSEL. A glass layer is used over the VCSEL/photoreceiver chip for protection, where microlens arrays for focusing and collimating the optical beam are placed. The Diffractive Optical Elements (DOE) plate is inserted between the VCSEL/photoreceiver chip and the optical substrate. The DOE comprises two sections. The first section is the VCSEL collimator, which is a hologram capable of collimating and steering VCSEL beams, while the second section acts as a lens relay that prevents the cavity beam from diverging as it propagates, and also maintains its diameter within an adequate range.

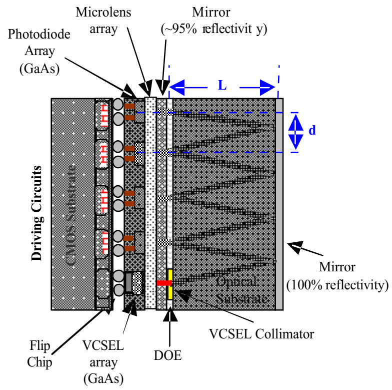

Fig. 2. True-time delay generation for the smart antenna.

The DOE in Fig. 2 is customarily coated to provide the desired reflectivity. As the in-cavity beam hits the DOE, a large portion of its power is reflected back inside the optical cavity while a small fraction of its power is transmitted through the DOE and the glass layer and then detected by one of the photoreceivers. For a cavity length L and photoreceiver spacing d, the incremental delay time between successive photoreceivers is

$$\Delta\tau = \frac{2n_o\sqrt{L^2 + (d/2)^2}}{c} \qquad (2)$$

where n_o is the refractive index of the optical substrate, and c is the speed of light in vacuum. The post amplifier of each photoreceiver element can independently be activated to produce either a delayed incoming signal or a zero output signal. An electronic combiner adds (or subtracts) the amplified photocurrents to generate the sum of many delayed versions of the signal.

Simulation and Experimental Results

Fig. 3 shows the simulated azimuth gain patterns for a 5.6GHz 7-element antenna employing a 64-tap delay for each antenna element. The spacing between the antenna elements is half the RF wavelength. The Minimum Mean-Square Error (MMSE) algorithm was used to generate null objectives at -45°, -10° and 45°, and desired beam directions at 60°, 15°, -30° and -50°.

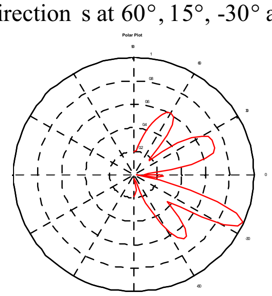

Fig. 3. The polar plot of 7-element Array Factor for the proposed MicroPhotonic smart antenna.

The experimental setup for the null beamformer is shown in Fig. 4, where multiple delayed optical beams with incremental true-time delay of 10ns were generated. The mean diameter of the detected optical beams was about 70µm and their spacing was 250µm as shown in Fig. 5. This spacing was chosen to enable the use of standard photodiode arrays for optical to electrical conversion.

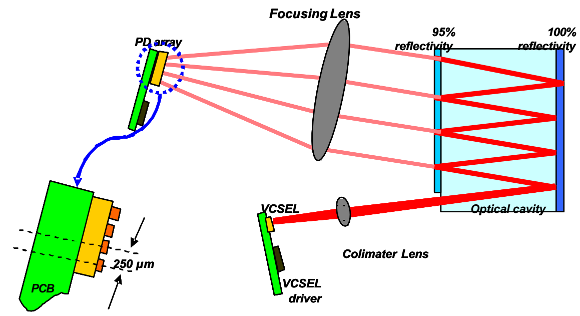

Fig. 4. Experimentalsetup for demonstrating the priciple of the MicroPhotonic smart antenna.

In Fig. 5 the measured delayed optical beams were captured by an infra-red camera. Note that a uniform beam spacing is maintained, however, a slight beam divergence is exhibited as the optical beam propagates within the optical cavity. This can be overcome by using a DOE as illustrated in Fig. 2.

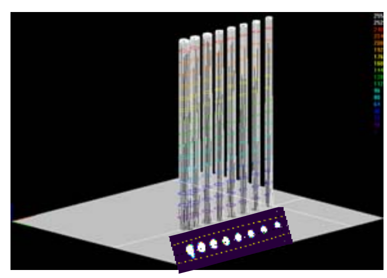

Fig. 5. Measured delayed optical beams emerging from the true-time delay unit.

Conclusions

The design and assembly of a MicroPhotonic phased-array beamformer has been described. The key building blocks of the MicroPhotonic beamformer have already been fabricated. Simulation and proof-of-concept experiments have demonstrated the principle of the beamformer for a 5.6GHz operation band.

References

1. Zmuda, H et al., Fibre & Integrated Optics 19 (2000) pp. 137-154.
2. Kamal Alameh et al, 2nd IEEE International Workshop on Electronic Design, Test & Applications (2004) p. 208.
3. Mark Taublenbatt, Executive Symposium on Photonics Commercialization, IBM Corp (2006).